Nature of the surface-reconstruction phase transition and the high-temperature phase of clean W(001)

L. D. Roelofs*
Fritz-Haber-Institut der Max-Planck-Gesellschaft, Faradayweg 4-6, D-1000 Berlin 33, Federal Republic of Germany

J. F. Wendelken
Solid State Division, Oak Ridge National Laboratory, Oak Ridge, Tennessee 37831
(Received 12 March 1986)

A short-range model for the W(001) reconstruction phase transition is presented and its properties are analyzed by means of a Monte Carlo calculation. The latter determines ordering properties as well as properties that reveal the local character of the atomic displacements, including the integer-order diffraction beams and distributions of displacements. New measurements of the behavior of the integer beams through the transition are also presented and interpreted in terms of the simulation results. The question of the character of the transition, displacive or order-disorder, is discussed from the perspective in which those two possibilities are limiting cases. Variation along this spectrum is determined by important physical characteristics of the electronic driving force. Implications of our results for the proper understanding of the Debye-Waller behavior of W(001) and for measurements of critical exponents in this system are also discussed.

I. INTRODUCTION

Although tungsten is not a material of unusual technological importance, and its surfaces do not seem to have significant potential for catalysis or interesting surface reactions, there have been an amazing number of studies of its (001) surface especially. (For a summary of this work see Refs. 1–3.) This great interest has been sparked mostly by the subtle reconstruction phase transition exhibited by this surface, which has encouraged the testing of new theoretical and experimental techniques on a very challenging, almost notorious, problem.

Notwithstanding this great dedication, progress toward an understanding of the driving force for the reconstruction and toward agreement on the nature of the phases and transition has not been rapid. Recently, however, at least the former issue seems to have been clarified.[1] The suggestion of Terakura *et al.*[4] (based on parametrized tight-binding calculations), that the mechanism involves states throughout the *d* band and amounts to a very short-range driving force, has been borne out by more sophisticated, first-principles, total-energy calculations.[5,6]

Simultaneously, consensus is emerging regarding the character of the transition and high-temperature (HT) phase (the earlier controversy—not yet entirely resolved—and the current picture will be outlined below) and these are consistent with qualitative expectations for a short-range driving force and simulation results based on a simplified model.[7] Thus it now seems appropriate to extend the study of Ref. 7 to a model with the full symmetry of the surface allowing: (i) further clarification of the nature of the transition and HT phase; (ii) direct confrontation with new experimental studies using low-energy electron diffraction (LEED)—also included in this paper—of the long-range order and local disorder of the surface atom displacements; (iii) determination of sensitivity of measurable parameters to variation in model parameters; and (iv) quantitative study of perturbations of the system due, for example, to adsorption,[3,8–10] or to the presence of uniformly spaced, oriented surface steps.[11–14] The present study, including the following paper, addresses these issues by means of a Monte Carlo simulation, which is used to calculate quantities appropriate for full characterization of the phases throughout the temperature range of interest and for elucidating the energetics of the transition.

A. Nature of phases and phase transition

The character of the clean, reconstructed phase (to be denoted LT, for low temperature) was first deduced by Debe and King[15,16] on the basis of an elegant symmetry argument, and later verified by Barker *et al.*[17] using dynamical LEED calculations. The surface layer atoms displace along the diagonal directions in the surface plane, exhibiting long-range $c(2\times2)$ order as shown in Fig. 1(d). The most extensive LEED study to date, that of Walker *et al.*,[18] gives a displacement magnitude at temperature $T=200$ K [$T_c\simeq210$ K (Ref. 14)] of 0.16 Å, in good agreement with the calculation of Fu *et al.*[6] which for the same structure finds a total energy minimum at displacement magnitude $u_0=0.18$ Å.[19] [The correspondence is further improved by the implication in our model calculation that the average displacement magnitude should decrease between $T=0$ (total energy minimum) and the vicinity of the phase transition.]

The characters of the phase transition and HT phase were initially controversial, although some convergence has now occurred. Debe and King[16] initially suggested that the transition has order-order character and the HT

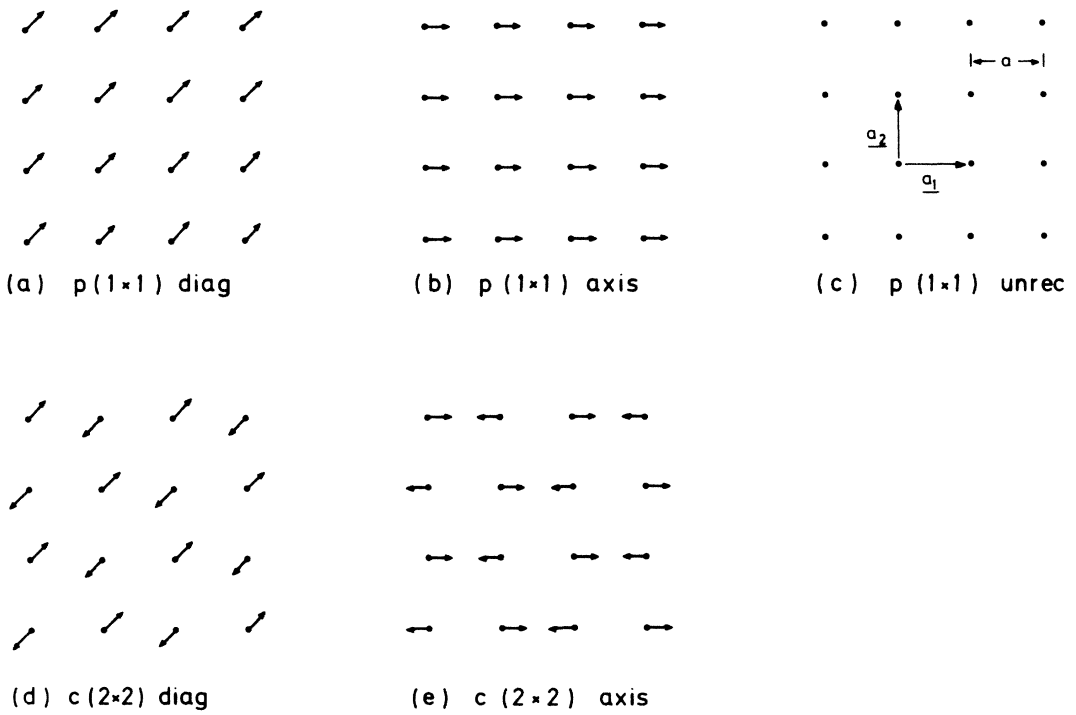

FIG. 1. Possible (001) surface displacive ordered states of (a)–(c) $p(1\times1)$ and (d)–(e) $c(2\times2)$ character. Designations "diag" and "axis" refer to the orientation of the displacements.

phase has $p(1\times1)$ bulk termination character [Fig. 1(c)] with displacement magnitudes typical of thermal vibrations at the appropriate temperature. (At room temperature one might estimate a root-mean-square amplitude of $\rho_{\text{surf}}=0.07\pm0.02$ Å.[20]) King[2] has recently summarized the arguments for this view, and mentions another possible ordered form for the HT phase, that of Fig. 1(b), first mentioned by Debe and King.[21] A third ordered possibility, that of Fig. 1(a), was suggested by Walker *et al.*[18] Barker and Estrup,[22] on the other hand, have suggested a *disordered* character for the HT phase in which individual atoms retain displacement amplitudes comparable to those below T_c, but lose long-range order.

It has been realized for some time from related work in the theory of structural phase transitions[23,24] that for a short-range driving force the HT phase must have disordered character in the immediate vicinity of the transition.[1,7,25] "Vicinity of the transition" means the temperature range where the correlation length ξ of $c(2\times2)$ fluctuations remains significantly greater than the W lattice constant.

Well above T_c (including room temperature) theoretical indications are lacking and experimental evidence is difficult to interpret conclusively (see below), so the situation is less clear. The important characteristics of local disorder in terms of theoretical impact are (i) the mean-square amplitude, (ii) degree of short-range correlation, and (iii) the details of the distribution of displacements, which varies between the displacive limit—Gaussian distribution of width typical of thermal displacements[20]—and the disordered limit—a highly anharmonic distribution with well-localized maxima at displacement magnitude similar to that in the low-temperature (LT) phase not too far below T_c. In this temperature regime the various viewpoints[1,2,7,22,25] are not too well defined, but significant differences probably remain with Refs. 1 and 2 favoring the displacive picture and Ref. 22 inclining toward the disordered picture. Unfortunately, these differences are of considerable consequence for both theory (see, e.g., Ref. 26) and interpretation of experiment. In fact, the lack of firm experimental evidence for the character of the HT phase, which bespeaks the limited ability of most probes to determine the degree of local disorder on a surface, is due in large part to that consequence. We illustrate this point by briefly discussing the sensitivity of various popular surface techniques for determining the degree and nature of structural disorder.

B. Experimental sensitivity to disorder

There are several dynamical LEED studies of the HT phase (a list appears in Ref. 21). Although the energy dependence of diffraction peak intensities is, in principle, sensitive to disorder, the technique fails in practice due to the difficulty of calculating comparison spectra for disordered models. The direct approach is unfeasible due to lack of symmetry, and the only alternative technique for handling disorder[27] is suitable only for Debye-Waller-type, i.e., fully uncorrelated, Gaussian-distributed disorder.

There are also recent studies[28,29] of the surface $4f_{1/2}$ core levels. Beginning in the HT phase the shifts of these levels attendant upon H-adsorption[29] to produce the $c(2\times2)$-H phase,[30] and upon cooling[28] into the LT phase

were measured. The shift is one-third as large in the case of the latter. Interpretation of these shifts is, however, subtle, requiring first a structural model (presumably containing appropriate disorder) and then accurate calculation of the local density of states. (We note in passing that the smallness of the measured shifts between the HT and LT phases could not be reconciled in Ref. 28 with model calculations. This may have been a consequence of the assumption of an *ordered, undisplaced* HT phase. As the core levels are sensitive to the local environment of the atom, one expects that the assumption of a disordered HT phase, if the calculations could be carried out, would have led to a smaller shift.)

One faces the same intrinsic difficulty in searching for evidence of disorder in measurements of occupied states nearer the Fermi level.[31,32] Calculating surface band structures is challenging enough for fully ordered structures. Incorporation of realistic surface layer disorder involves an intractable loss of symmetry. (Campuzano *et al.*[31] have suggested that a significant degree of disorder would smear out surface states near $\overline{M}$, although to the present authors' knowledge, the effects of disorder on this scale—about 5–7 % of the lattice constant—have not been investigated.)

Work-function changes have also been measured,[16,33] but the variation is small and is not concentrated near the transition.[33] In any case, the connection to surface disorder is unclear.

Ion scattering[34] is directly sensitive to surface layer disorder, but interpretation requires a simulation in which the details of the disorder, i.e., the degree of correlation and the shape of the displacement distribution, obviously play a role.[35] Significantly, the study of Stensgaard *et al.*[34] indicates that there is little difference in the number of displaced atoms between the HT and $c(2\times2)$-H phase and in the latter all the atoms in the surface layer are thought to be displaced.[2,22]

Diffraction measurements throughout the surface Brillouin zone do offer information on the order of intermediate range, and as pointed out by Debe and King,[16] the temperature dependence of the integer beams is related to local disorder, although, as pointed out in Refs. 22 and 33 and established in detail in the present work, existing analyses[2,16] are not adequate. Multiple scattering, of course, complicates detailed study of disorder by this approach.

The above catalog establishes both the importance of accounting for disorder in interpreting experiments and the (related) difficulty of experimentally characterizing the disorder. However, the last mentioned approach does seem to hold some promise. Thus, a main part of the present work is devoted to new measurements of the temperature dependence of diffraction intensities throughout the Brillouin zone, including the background and integer-beam intensities, and a careful analysis of these variations in the kinematic approximation. Our study establishes the experimental basis for a disordered HT phase. In addition, by establishing the sensitivity of the character of the HT phase to some aspects of the physics of the driving force, we offer some indications concerning the latter. We also find that the Debye-Waller factor behaves anomalously for this system, this having implications for critical exponent studies.[14] By introducing a very general short-range, small-displacement model we also can assess the effect of perturbations due to low coverage adsorption[3,8–10] and reduce the parameter space of such models by (rigorous) elimination of the $T=0$ displacement magnitude as an independent variable. Finally, we also model the effect of oriented steps on the transition. This study is presented according to the following outline.

In Sec. II the general short-range interaction, small-displacement model is introduced and analyzed qualitatively. Two sets of choices for model parameters, meant to be representative for the range of possibilities for the actual system, are given. In Sec. III we describe our Monte Carlo code and the "observables" it calculates. In Sec. IV we display our Monte Carlo results for the behavior of both models over an extensive temperature range, $T=0$ to $T=3T_c$. In Sec. V the experimental results are presented and discussed in the context of model simulation results. The anomalous Debye-Waller variation is also noted there. In Sec. VI we present our conclusions and discuss the limitations of this work. The following paper extends the study to assess the effects of perturbations due to low-coverage adsorption and oriented surface steps. Some further aspects of our study pertaining to the total energy-surface atom and a comparison with first-principles calculations[4–6] have been included in another work.[36]

II. SHORT-RANGE MODEL

Our model for the energetics of the W(001) reconstruction has been described before,[3,9] but appears in more general form here. The model is two-dimensional with the energy written in terms of $\{\mathbf{u}_i\}$, the displacements in the surface plane of surface layer W atoms. In the real surface the motion in the direction perpendicular to the surface does not exhibit $c(2\times2)$ order.[37] There may of course be a relaxation of the entire layer inward or outward, and there will certainly also be vibrational motion in this direction. However, neither of these affect either the character of the transition or that of the ordered phase, and therefore we have not included z-component displacements in our model.

The model includes short-range interactions between nearby surface W atoms and a local potential for each W atom which can be thought of as arising from underlaying layers in the crystal. The evidence for a short-range driving force is summarized in Refs. 1, 7, and 9. The local potential is discussed in more detail below. In this section we introduce these two contributions to the Hamiltonian and develop a convenient set of parameters using the symmetry of the surface to restrict their number as much as possible.

A. Interaction terms

It is convenient to describe the short-range interactions in terms of (2×2) dynamical matrices:

$$H_I = \sum_{\langle ij\rangle_1} \sum_{\alpha,\beta} u_{i\alpha}\Phi_{\alpha\beta}(\mathbf{R}_i - \mathbf{R}_j)u_{j\beta} + \sum_{\langle ij\rangle_2} \sum_{\alpha,\beta} u_{i\alpha}\Phi_{\alpha\beta}(\mathbf{R}_i - \mathbf{R}_j)u_{j\beta} , \quad (2.1)$$

where $\langle ij\rangle_1$ denotes the set of nearest-neighbor (NN) pairs of sites and $\langle ij\rangle_2$ the set of next-nearest-neighbor (NNN) pairs. The vector $\mathbf{R}_i$ is the location of bulk termination site i. The sums on α and β range over the x and y components. We take the basis vectors of the surface to be $\mathbf{a}_1 = a\hat{\mathbf{x}}$ and $\mathbf{a}_2 = a\hat{\mathbf{y}}$ so that the NN dynamical matrices are $\Phi(\pm\mathbf{a}_1)$ and $\Phi(\pm\mathbf{a}_2)$, and the NNN dynamical matrices are $\Phi(\pm\mathbf{a}_1 \pm \mathbf{a}_2)$. The square symmetry of the surface restricts the forms of these matrices. Consider first the NN dynamical matrix $\Phi(\mathbf{a}_1)$. Off-diagonal elements may not appear in this term since a surface with just this term has a mirror plane in the y direction. The transformation $u_{ix} \rightarrow -u_{ix}$ for all i changes the sign of off-diagonal terms, which therefore must vanish. For later convenience we thus take

$$\Phi(\pm\mathbf{a}_1) = \begin{bmatrix} J_1 + K_1 & 0 \\ 0 & J_1 - K_1 \end{bmatrix} . \quad (2.2a)$$

$\Phi(\pm\mathbf{a}_2)$ must also be diagonal, and by noting that fourfold rotations connect $\Phi(\mathbf{a}_1)$ and $\Phi(\mathbf{a}_2)$ we find that

$$\Phi(\pm\mathbf{a}_2) = \begin{bmatrix} J_1 - K_1 & 0 \\ 0 & J_1 + K_1 \end{bmatrix} . \quad (2.2b)$$

Thus the nearest-neighbor interaction can be seen to be the sum of two parts: a dot-product term

$$\Phi_J(\pm\mathbf{a}_1) = \Phi_J(\pm\mathbf{a}_2) = \begin{bmatrix} J_1 & 0 \\ 0 & J_1 \end{bmatrix} , \quad (2.3a)$$

and a twofold term,

$$\Phi_K(\pm\mathbf{a}_1) = -\Phi_K(\pm\mathbf{a}_2) = \begin{bmatrix} K_1 & 0 \\ 0 & -K_1 \end{bmatrix} . \quad (2.3b)$$

We defer the detailed discussion of the character of these terms to Sec. II C. The NNN interaction can be similarly restricted and decomposed into

$$\Phi_J(\pm\mathbf{a}_1 \pm \mathbf{a}_2) = \begin{bmatrix} J_2 & 0 \\ 0 & J_2 \end{bmatrix} \quad (2.4a)$$

and

$$\Phi_K(\pm(\mathbf{a}_1 + \mathbf{a}_2)) = -\Phi_K(\pm(\mathbf{a}_1 - \mathbf{a}_2)) = \begin{bmatrix} 0 & K_2 \\ K_2 & 0 \end{bmatrix} , \quad (2.4b)$$

where Eq. (2.4a) is evidently another dot-product term, while the more complicated Eq. (2.4b) will be discussed in Sec. II C.

Thus, the most general form for NN and NNN pairwise interactions on this surface is seen to be describable in terms of only four parameters, J_1, K_1, J_2, and K_2 as defined in Eqs. (2.3) and (2.4).

B. Local terms

A second necessary ingredient in our model is a local term which can be thought of as arising from the interactions of an individual surface atom displacement with the underlying layers of the W crystal. Again we begin by determining what sorts of terms are allowed by symmetry. The local terms have the symmetry of the undistorted surface so that we can describe the local part with complete generality:

$$V(\mathbf{u}_i) = \tfrac{1}{2}Au_i^2 + \tfrac{1}{4}\tilde{B}u_i^4 + \tfrac{1}{2}C(u_{ix}^4 + u_{iy}^4) , \quad (2.5)$$

including all possible terms up to fourth order in the displacements. The restoring forces, i.e., the fourth-order terms, are put in V since the second-layer atoms, being the closest, are the most responsible for the repulsive stabilizing force.

C. Ordered states and the effect of the interaction terms

It is useful to begin by examining the angular dependence of V. Let θ_i be the angle relative to $\mathbf{a}_1$ (see Fig. 1) made by $\mathbf{u}_i$. Then we can separate the last term in Eq. (2.5) into a contribution independent of θ_i and one which describes the variations of V versus θ_i. Then V becomes

$$V(\mathbf{u}_i) = \tfrac{1}{2}Au_i^2 + \tfrac{1}{4}Bu_i^4 - \tfrac{1}{2}V_4u_i^4\cos(4\theta_i) , \quad (2.6)$$

where $B = \tilde{B} + \frac{3}{2}C$ and $V_4 = -\frac{1}{4}C$.

The total Hamiltonian $H = H_I + V$ [Eqs. (2.1) and (2.6)] is general in that it is appropriate for any surface of square symmetry with short-range interactions, at most small displacements and a relatively inactive bulk. Depending on the values of the parameters (which could in principle be extracted from a sufficiently accurate, first-principles total-energy electronic structure calculation) many possible behaviors ranging from a nonreconstructed ground state to incommensurate phases can be realized by this model. The former occurs, for example, when A is positive and sufficiently large (see below) to dominate the J and K interaction terms. We are more interested, however, in parameter choices that lead to a reconstructed ground state.

With the local potential of Eq. (2.6) it is clear that one of two possible sets of displacement directions must be favored, $\{0, \pi/2, \pi, 3\pi/2\}$ (axis) or $\{\pi/4, 3\pi/4, 5\pi/4, 7\pi/4\}$ (diag), the former if $V_4 > 0$ and the latter if $V_4 < 0$. The other two terms of (2.6) and the J-type interaction terms, Eqs. (2.3a) and (2.4a) are independent of absolute angle. The remaining interactions, Eqs. (2.3b) and (2.4b), are also consistent with either of the above sets, and so all possible fully ordered states can be constructed with displacements chosen either along the axes or along the diagonals. These states are tabulated in Figs. 1 and 2, carrying in each case a designation of "diag" or "axis" as appropriate. The interactions must determine the character of the order that develops. Table I displays this connection. The designation "un" denotes "uncoupled," i.e., the interaction makes no contribution to the ordered-state energy. "Favor" indicates that the energy of the particular ordered state decreases in proportion to the strength of the associated parameter and "oppose" denotes the reverse.

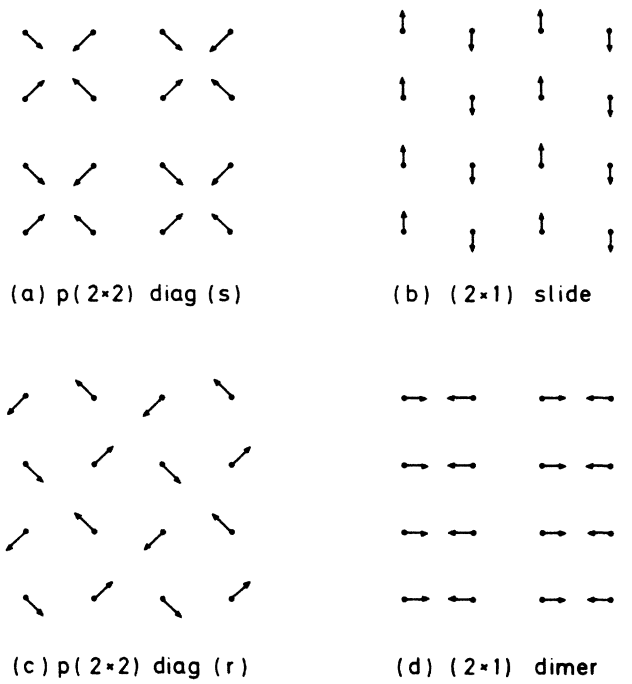

FIG. 2. Possible (001) surface ordered states of (2×1) and (2×2) character. States (a) and (c) can be experimentally distinguished via the glide plane present only in (c). The designations s and r denote "squeeze" and "rotate."

As we wish our model to describe clean W(001) which has $c(2\times2)$-diag character at low temperature, we clearly must choose J_1-J_2 to be positive and the other parameters, K_1 and K_2, not to be large in magnitude, since they tend to induce ordered states of incorrect character. The states induced by Φ_K (NNN) (in the unlikely event of it being dominant over the NN interactions) are like those induced by Φ_K (NN) (hence our notation which emphasizes their similar character) except that they occur on one $c(2\times2)$ sublattice of the surface. They thus have $2(\sqrt{2}\times2\sqrt{2})R45°$ and $(\sqrt{2}\times2\sqrt{2})R45°$ symmetry.

The model whose study is the main subject of this paper has been chosen to have $J_2=K_1=K_2=0$ and $J_1>0$ so that the latter term is responsible for driving the transition. Although this choice appears somewhat arbitrary, taking one or more of J_2, K_1, and K_2 to be nonzero would not change the qualitative aspects of the transition so long as they are not comparable in magnitude to J_1 (see next paper).

This is not to suggest that the terms J_2, K_1, and K_2 are not important. We have previously noted[9,10] that the effect of an adsorbate at low coverage on the transition can be understood as a variation proportional to the adsorbate coverage of these terms. For example, bridge-site adsorption increases J_1, and tends therefore to enhance the reconstruction.[3,9] On the other hand, adsorption into the hollow site leaves J_1 unaffected but increases J_2, K_1, and K_2 in the positive direction.[10] In Ref. 10 it was suggested that an increase in J_2 opposes the $c(2\times2)$ order, while the increases in K_1 and K_2 would have little effect due to the absence of coupling. The following paper verifies these suggestions and also demonstrates via explicit simulation that including J_2, K_1, or K_2 in the model up to a strength of $\frac{1}{2}J_1$ does not alter the character of the transition. Meanwhile it seems safe to base a qualitative study of the transition on the choice $J_1>0$, $J_2=K_1=K_2=0$.

D. Parameter choices for the local potential

We must still specify the parameters of the local potential and here one might expect the choices to have a more significant effect on the qualitative character of the transition and HT phase.

For example, there is first the question of whether there are wells in the local potential at nonzero displacement. This would occur if A were chosen to be negative in Eq. (2.6). Note that B must in general be positive to keep the individual $\mathbf{u}_i$s bounded. In terms of physical implications this would mean that a significant part of the driving force of the reconstruction arises from coupling between electronic states in the surface layer with those in the second and deeper layers. There is some experimental evidence from photoemission studies[31,32] supporting an effect from coupling to the second layer. A surface resonance which crosses the Fermi energy near the point $(\pi/a,\pi/a)$ in the surface Brillouin zone was found to be even with

TABLE I. Coupling between order of various types and the interactions included in the model. "diag" and "axis" refer to all possible fully ordered states that can be constructed with displacements chosen either along the axes or the diagonals. "un" denotes "uncoupled," i.e., the interaction makes no contribution to the ordered-state energy. "Favor" indicates that the energy of the particular ordered state decreases in proportion to the strength of the associated parameter and "oppose" denotes the reverse.

		$p(1\times1)$	$c(2\times2)$	$p(2\times2)$diag(s)	$p(2\times2)$diag(r)	(2×1)slide	(2×1)dimer
Φ_J(NN)	$J_1<0$	favor	oppose	un	un	un	un
	$J_1>0$	oppose	favor	un	un	un	un
Φ_K(NN)	$K_1<0$	un	un	oppose	favor	favor	oppose
	$K_1>0$	un	un	favor	oppose	oppose	favor
Φ_J(NN)	$J_2<0$		favor	oppose	oppose	oppose	oppose
	$J_2>0$		oppose	favor	favor	favor	favor
Φ_K(NNN)	$K_2<0$		un	un	un	un	un
	$K_2>0$		un	un	un	un	un

TABLE II. Parameter choices for two models.

Model	J_1	A	B	V_4	r	s	u_0
I	1.0	−8	+8	−2	−2	$\frac{1}{2}$	$\sqrt{3}$
II	1.0	1	5	−2	$\frac{1}{4}$	$\frac{4}{5}$	$\sqrt{3}$

respect to reflection through the mirror place containing the displacement direction.[32] A state of even symmetry would couple more readily to an atom in the direction of the nearest second-layer atom than to the nearest surface-layer atom.

Inglesfield,[1] however, points out that most theoretical studies emphasize the importance of a band of states of odd symmetry [which cross the Fermi level closer to $(\pi/a,\pi/a)$ in theoretical studies[5,26] than in experiment[31,32]] which would be more consistent with interactions between surface layer atoms. It seems relevant to add, on the other hand, that the recent calculation of Fu *et al.*[6] demonstrates a "bonding enhancement between surface and subsurface atoms," that Ohnishi *et al.*[26] explicitly display states involved in significant bonding between first- and second-layer atoms, and that the observed inward relaxation of the surface layer,[18] also suggests an interaction with the second layer.

If interactions with the second layer are not significant, the local potential should be taken to lack wells at finite displacement and would provide only a restoring force. Clearly this choice may affect the local character of the phases, and might even cause a difference in transition order.

Given the present uncertainty, to delineate sensitivity to this characteristic we have adopted two choices for the parameters of the local potential. These choices we term models I and II and they are given explicitly in Table II. Model I has a local potential with minima at finite displacement and is shown in Fig. 3(a). Model II lacks wells [see Fig. 3(b)], but retains the anisotropy favoring diagonal displacements required by experiment.

E. Elimination of u_0

The model as it now stands has four parameters: J_1, A, B, and V_4. It is possible to reduce the number of independent parameters to two without further approximation by noting that u_0, the equilibrium zero-temperature displacement magnitude, serves only as an integration scale factor in statistical averages. We are currently considering the Hamiltonian:

$$H = J_1 \sum_{\langle ij \rangle_1} \mathbf{u}_i \cdot \mathbf{u}_j + \sum_i \tfrac{1}{2} A u_i^2 + \tfrac{1}{4} B u_i^4 - \tfrac{1}{2} V_4 u_i^4 \cos(4\theta_i) \, . \tag{2.7}$$

We note first of all that H has the symmetry

$$H(-V_4) = H(V_4) \, , \tag{2.8}$$

since changing the sign of V_4 and rotating all the $\mathbf{u}_i$'s by 45° brings H back into its original form. We can thus

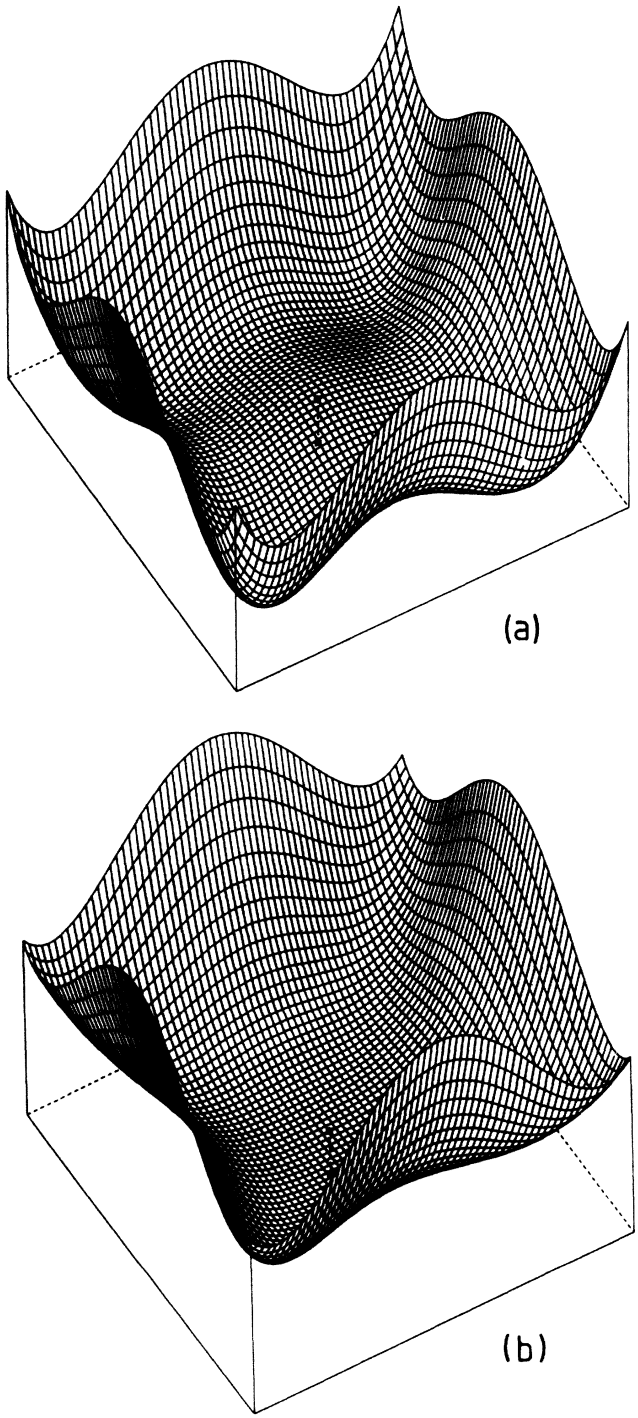

FIG. 3. Plot of assumed local potentials for (a) (top) model I and (b) (bottom) model II. $V(u_x,u_y)$ is represented by the vertical direction and the square beneath each plot is oriented with its edges along the ⟨100⟩ and ⟨010⟩ directions.

take V_4 to be negative, favoring diagonal displacements without loss of generality. H is also invariant with respect to the usual ferromagnetic-antiferromagnetic transformation, in which we take $\mathbf{u}_i \rightarrow -\mathbf{u}_i$ for all i on one $c(2\times2)$ sublattice and simultaneously change the sign of J_1. Thus the model needs to be studied for only one choice of sign for J_1, which we shall take to be positive, favoring the order of Fig. 1(d). It is worth emphasizing, however, that because of the above two symmetries, our study has a broader application than just to the transition between the LT and HT phases. For example the same surface with H coverage in the range (0.11—0.25) exhibits an ordered phase like Fig. 1(e),[22] describable by the same model but with $V_4>0$. Thus our study can be readily applied to that case. Another case would be the disordering of a uniformly displaced phase such as that of Fig. 1(a) or 1(b). Such structures have recently been proposed for the clean Pd(110) surface (rectangular symmetry) and for the H/W(110) system (centered rectangular symmetry).[38]

Next we take advantage of eliminating the length scale. The zero-temperature equilibrium displacement u_0 is obtained trivially from Eq. (2.7) as the (uniform) magnitude of displacements that minimizes the energy. In consequence of our choice of signs for J_1 and V_4 we choose $c(2\times2)$ displacements in the diagonal direction, and find the energy per site to depend on the displacement u as follows:

$$E(u)=-2J_1u^2+\tfrac{1}{2}Au^2+\tfrac{1}{4}Bu^4+\tfrac{1}{2}V_4u^4\ , \tag{2.9}$$

so that the minimum occurs at

$$u_0=[(4J_1-A)/(B+2V_4)]^{1/2}\ . \tag{2.10}$$

The energy per site at $u=u_0$ is

$$E_0=E(u_0)=-\frac{1}{4}\frac{(4J_1-A)^2}{B+2V_4}$$

$$=-\tfrac{1}{4}(4J_1-A)u_0^2 \tag{2.11a}$$

$$=-J_1u_0^2(1-r) \tag{2.11b}$$

where $r=A/4|J_1|$.

Another expression for E_0 is

$$E_0=-\tfrac{1}{4}(B+2V_4)u_0^4$$

$$=-\tfrac{1}{4}Bu_0^4(1-s)\ . \tag{2.11c}$$

where $s=2|V_4|/B$. (We have defined r and s to reflect the symmetries $V_4\rightarrow-V_4$ and $J_1\rightarrow-J_1$.) Equation (2.10) reveals conditions on the parameters that must be respected in order for the model to display the phenomena attributed to W(001). First, to have the reconstruction at all we require $4|J_1|-A>0$ ($r<1$). To keep the individual displacements bounded we require $B>0$ and $B-2|V_4|>0$ ($0<s<1$). The partition function, which we write here for a system with N sites, is

$$Z=\int d^2u_1\int d^2u_2\cdots\int d^2u_N\exp[-(1/kT)H]\ , \tag{2.12}$$

with H as in Eq. (2.7) and k and T being Boltzmann's constant and the temperature, respectively, and indeed any observable can be written in the form of such an integration. It is advantageous to change variables in this integration to a dimensionless length variable

$$\mathbf{w}_i=\mathbf{u}_i/u_0\ , \tag{2.13}$$

so that

$$Z=(u_0^2)^N\int d^2w_1\int d^2w_2\cdots\int d^2w_N\exp\left[-\frac{1}{kT}\left[J_1u_0^2\sum_{\langle ij\rangle_1}\mathbf{w}_i\cdot\mathbf{w}_j+\tfrac{1}{2}Au_0^2\sum_i w_i^2+\tfrac{1}{4}Bu_0^4\sum_i w_i^4 -\tfrac{1}{2}V_4u_0^4\sum_i w_i^4\cos4\theta_i\right]\right]\ . \tag{2.14}$$

Using Eqs. (2.11b) and (2.11d) we find

$$Z=u_0^{2N}\int d^2w_1\int d^2w_2\cdots\int d^2w_N\exp\left\{\frac{E_0}{kT}\left[\frac{1}{1-r}\sum_{\langle ij\rangle_1}\mathbf{w}_i\cdot\mathbf{w}_j+\frac{2r}{1-r}\sum_i w_i^2+\frac{1}{1-s}\sum_i w_i^4[1+s\cos(4\theta_i)]\right]\right\}$$

$$=u_0^{2N}\int d^2w_1\int d^2w_2\cdots\int d^2w_N\exp\left\{-\frac{1}{\tilde{T}}\left[\sum_{\langle ij\rangle_1}\mathbf{w}_i\cdot\mathbf{w}_j+2r\sum_i w_i^2+\left[\frac{1-r}{1-s}\right]\sum_i w_i^4[1+s\cos(4\theta_i)]\right]\right\}, \tag{2.15}$$

where

$$\tilde{T}=\frac{kT(1-r)}{(-E_0)}=\frac{kT}{J_1u_0^2}\ . \tag{2.16}$$

Inspection of Eq. (2.16) reveals that we have reduced the number of independent parameters to two (r and s), by scaling the temperature according to Eq. (2.16) and pulling the length-scale factor out of the integral. This

means that a study of the Hamiltonian for one choice of the original four parameters can be trivially extended to all other choices of parameters that are consistent with the same values of r and s (Table II also lists the values of r and s for our models I and II). For example, our study of model II thus can be applied to any choice of model parameters that satisfy the relations $A=|J_1|$ and $V_4=\pm\frac{2}{5}B$. One merely adjusts the temperature scale in accord with Eq. (2.16).

III. MONTE CARLO CALCULATION

In this section the particulars of the Monte Carlo calculation are given. We use the standard Metropolis algorithm.[39] This method has been applied most often to systems whose fundamental degrees of freedom are discrete,[40] but has also been used less frequently in the continuous case.[7,41] Since the method is well-proven and fairly standard, we describe only the observables calculated and our choices for lengths of runs, etc.

A. Monte Carlo parameters

Except in our study of the effect of steps on the transition, we used periodic boundary conditions. The sizes of lattices studied were 12×12, 24×24, and 48×48. The length of runs varied since we were interested in the behavior not only close to the transition, where convergence times are long, but also well away from T_c, where they are comparatively short. Typically in the latter case we used 5000—20 000 move attempts per surface atom (hereafter simply "MC steps" for Monte Carlo steps), and near T_c we used 40 000—100 000 MC steps. In all cases we discarded the first 10% of the MC steps to allow for equilibration. For both our models u_0 has the value $\sqrt{3}$. To ensure that the W(001) atoms could move between the minima in the potential, we considered separately random but simultaneous changes in u_{ix} and u_{iy} uniformly distributed in the interval $[-2.5,2.5]$. Under these conditions the rate of acceptances of the changes was about 17, 22, and 29% at 10% below T_c, T_c, and 10% above T_c, respectively, in the case of model I. The rates were comparable for model II, but slightly smaller below T_c. The execution time per MC step on a 24×24 lattice including calculation of observables every tenth step was about 0.3 CPU (central processing unit) seconds on a CDC Cyber 175.

B. Averages

During a Monte Carlo " experiment" one can calculate average values for any observable expressible in terms of the configuration of the system. In order to compare our model with experiments on W(001) we have determined the average values and variances of several energetic and ordering observables of our model.

1. Order parameters and half-order (kinematic LEED features)

The kinematic LEED intensity at point $\mathbf{k}=(k_x,k_y)$ of the surface layer atoms is

$$I(\mathbf{k})=\left\langle\left|\sum_i \exp-i\mathbf{k}\cdot(\mathbf{R}_i+\mathbf{u}_i)\right|^2\right\rangle \tag{3.1}$$

$$=\left\langle\left|\sum_i \exp(-i\mathbf{k}\cdot\mathbf{R}_i)\exp(-i\mathbf{k}\cdot\mathbf{u}_i)\right|^2\right\rangle . \tag{3.2}$$

(Throughout this paper the notation $\langle\ \rangle$ denotes a partition function average implemented as an average over a Monte Carlo run.) For the purpose of comparison with experiment we are interested in the low-order, diffraction beams only. Since the equilibrium low-temperature displacements are known to be smaller than 0.2 Å,[18] $|(\mathbf{k}\cdot\mathbf{u}_i)|\ll1$ and we can expand the second exponential in Eq. (3.2). Hence,

$$I(\mathbf{k})\simeq\left\langle\left|\sum_i \exp(-i\mathbf{k}\cdot\mathbf{R}_i)[1-i\mathbf{k}\cdot\mathbf{u}_i-\tfrac{1}{2}(\mathbf{k}\cdot\mathbf{u}_i)^2]\right|^2\right\rangle \tag{3.3}$$

$$=\left\langle N^2\delta_{\mathbf{k},\mathbf{G}}+\left|\mathbf{k}\cdot\sum_i \mathbf{u}_i\exp(-i\mathbf{k}\cdot\mathbf{R}_i)\right|^2 -N\delta_{\mathbf{k},\mathbf{G}}\sum_i(\mathbf{k}\cdot\mathbf{u}_i)^2\right\rangle . \tag{3.4}$$

Equation (3.4) is valid to second order in $(\mathbf{k}\cdot\mathbf{u}_i)$. $\mathbf{G}$ denotes a reciprocal-lattice vector of the undistorted surface.

The half-order LEED features occur at $\mathbf{k}_0^{\pm}=(\pi/a,\pm\pi/a)$. Define

$$\mathbf{v}=\sum_i \mathbf{u}_i\exp(-i\mathbf{k}_0^{+}\cdot\mathbf{R}_i) . \tag{3.5}$$

($\mathbf{v}$ is a real vector since the phase factor only takes on values ±1.) Then

$$I(\mathbf{k}_0^{+})=\langle(\pi^2/a^2)(v_x+v_y)^2\rangle , \tag{3.6a}$$

$$I(\mathbf{k}_0^{-})=\langle(\pi^2/a^2)(v_x-v_y)^2\rangle . \tag{3.6b}$$

Thus to compare half-order LEED intensities with experiments we calculate the thermal averages $\langle(v_x+v_y)^2\rangle$, $\langle(v_x-v_y)^2\rangle$, and their variances. $I(\mathbf{k}_0^{+})$ is nonzero in the ordered phase when the displacements are along the [110] direction and $I(\mathbf{k}_0^{-})$ is nonzero when they are along the $[\bar{1}10]$. In a real experiment on a flat surface there are roughly equal numbers of domains in the two directions, so to facilitate comparison with experiment it is convenient to calculate the average of the two intensities in Eqs. (3.6):

$$I_{\mathrm{av}}(\mathbf{k}_0)=(\pi^2/a^2)\langle v_x^2+v_y^2\rangle . \tag{3.7}$$

Because of the unknown scattering power of W atoms, multiple scattering, and other complications, it is not possible to determine the absolute magnitude of these intensities. However, after normalization we can compare the temperature variations of these quantities with experiment in a straightforward way. These half-order intensities also contain the squares of the two component order parameters and therefore are a convenient way of extracting the order parameter values. (See, however, Sec. V B.)

2. Integer-order LEED features

A second item of experimental information by which we can assess our model is the behavior of the integer-order LEED features. We use Eq. (3.4) again this time with the **k** vectors of the (10) and (01) beams:

$$\Delta I(10)=\left\langle \left[\frac{2\pi}{a}\sum_i u_{ix}\right]^2 - N\sum_i \left[\frac{2\pi}{a}u_{ix}\right]^2 \right\rangle , \tag{3.8a}$$

$$\Delta I(01)=\left\langle \left[\frac{2\pi}{a}\sum_i u_{iy}\right]^2 - N\sum_i \left[\frac{2\pi}{a}u_{iy}\right]^2 \right\rangle , \tag{3.8b}$$

where ΔI is the *change* in the kinematic intensity due to the nonzero displacements. The first terms on the right-hand sides of Eqs. (3.8a) and (3.8b) are negligible in the ordered state, but above T_c are of order $N\langle u^2\rangle/a^2$,

$$\langle u^2\rangle=\left\langle \frac{1}{N}\sum_i u_i^2 \right\rangle , \tag{3.9}$$

while the second terms are of order $N^2\langle u^2\rangle/a^2$, and so dominate the change in intensity. The variation of the integer intensity is essentially determined by the variation of $\langle u^2\rangle$. Our Monte Carlo program also calculates the averages of the quantities defined in Eqs. (3.8) and (3.9) and their variances.

3. Features related to the energy

One of the key realizations emerging from our work stems from the coupling that occurs in this model between the local energy and the bonding energy. Therefore, we also calculate separate averages and variances of each term in Eqs. (2.1) and (2.6), and the average and variance of the total energy. These latter calculations are of some additional interest because they reveal the characteristic singularities that one would see in a study of the temperature dependence of the integrated half-order intensity through the transition.[42] Also, the separate expectation value of the bond energy, though not experimentally observable, is directly proportional to the nearest-neighbor correlation, an important quantity in characterizing the disorder. These results are discussed in Ref. 36.

4. Distribution of displacement magnitudes

At any given temperature we calculate the expectation value of the square magnitude of the displacements $\langle u^2\rangle$, but this by itself does not adequately define the character of the phase. It is useful to have in addition a determination of the characteristic spread of values of u^2 about its average. Therefore we also determine the time average of this spatial variance:

$$\langle \Delta u^2\rangle=\left\langle \left[\frac{1}{N}\sum_i u_i^4 - \left[\frac{1}{N}\sum_i u_i^2\right]^2\right]^{1/2} \right\rangle . \tag{3.10}$$

The ratio $\langle \Delta u^2\rangle/\langle u^2\rangle$ along with $\langle u^2\rangle$ itself characterizes the degree of local order at any point in the phase diagram. For a benchmark we note that a phase with the displacements distributed uniformly in the (u_x,u_y) plane out to a magnitude of u_0 would have $\langle u^2\rangle=\frac{1}{2}u_0^2$ and $\langle \Delta u^2\rangle/\langle u^2\rangle=1/\sqrt{3}=0.58$.

Since the calculation produces many equilibrium configurations of any given phase we can also accumulate histograms of displacement magnitudes at any point in the phase diagram.

IV. RESULTS

In this section we present the results of the Monte Carlo calculation described in the preceding section. A more extensive discussion follows in Sec. V.

A. Transition and high-temperature phase—model I

In both experiment (see Sec. V A) and simulation the phase transition can be seen either by observing the half-order beams or the integer beams, in the former as a dramatic drop in intensity to nearly zero and in the latter as a coincident (but smaller in magnitude) increase in intensity. Figure 4 shows our calculation using a 12×12 lattice of the temperature dependence of the average half-order intensity defined in Eq. (3.7), and the variation of the average (10) and (01) integer intensities as in Eqs. (3.8). (Because our model demonstrates diagonally oriented ordering, the two integer beams calculated always come

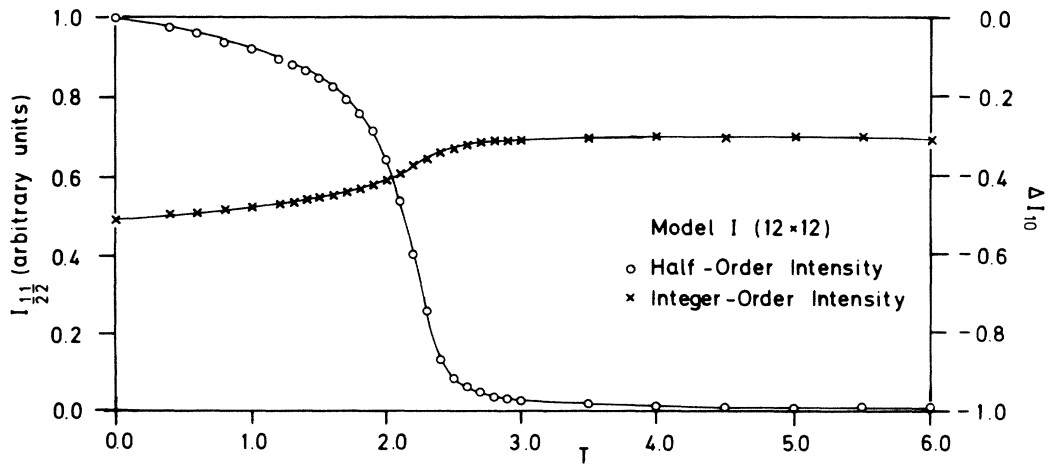

FIG. 4. Plots of simulated kinematic half-order intensity and decrease in integer-order intensity versus temperature for model I.

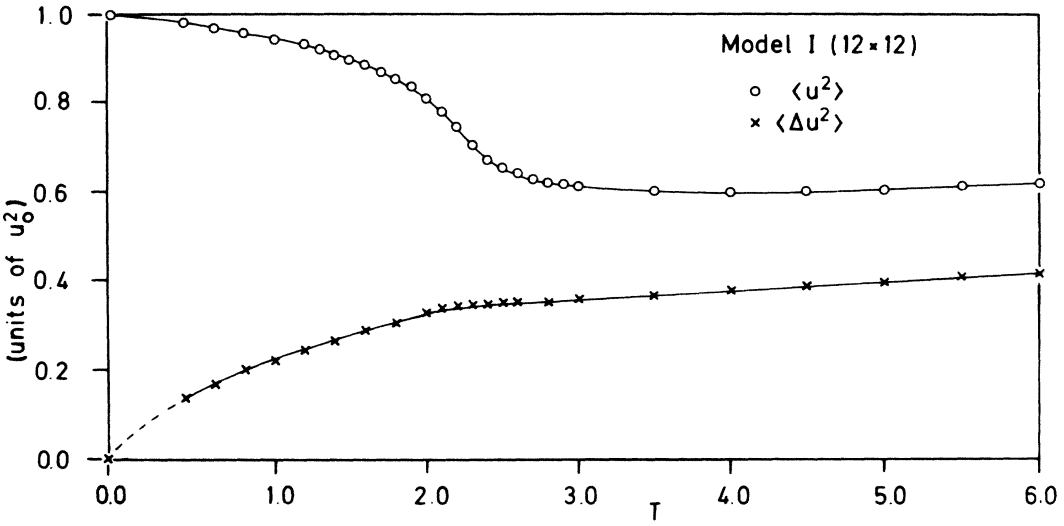

FIG. 5. Plots of stimulated average and variance of square displacement magnitude versus temperature for model I.

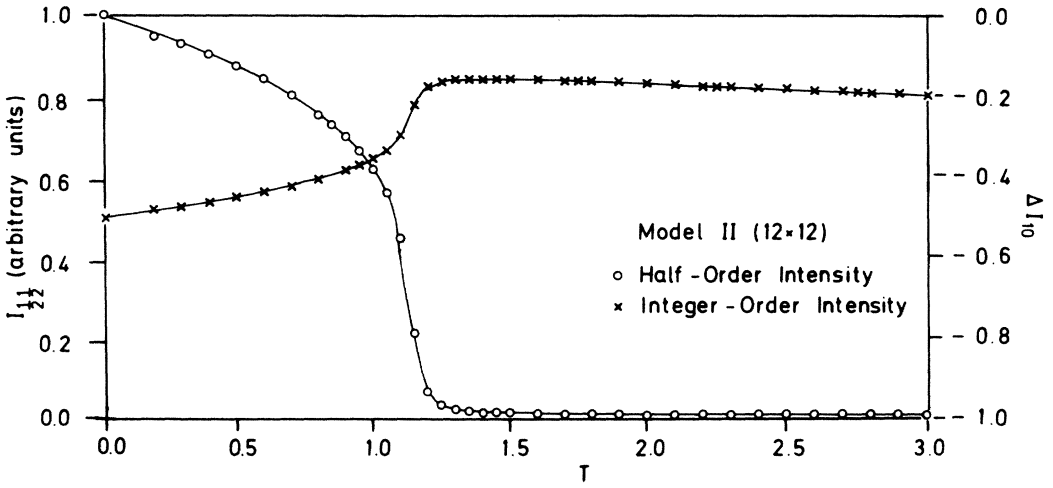

FIG. 6. Same as Fig. 4 for model II.

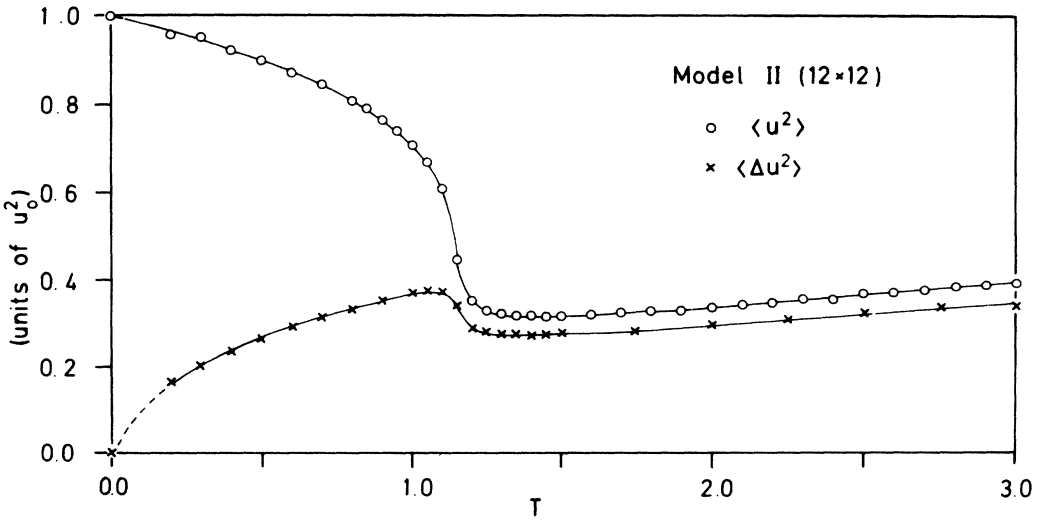

FIG. 7. Same as Fig. 5 for model II.

out very close, but not—because of statistical fluctuations—exactly equal in magnitude.) Some features of Fig. 4 which should be noted are (i) the half-order beams show an *apparent* Debye-Waller[27] decrease in intensity below the phase transition which occurs—located by the inflection point of the curve[42]—at $T_c = 2.20 \pm 0.05$ (all temperatures are given in units of J_1); (ii) some of this decrease in intensity is evidently contributing to an increase in the intensity of the integer beams; however, not all of it is, and the remainder is appearing as a diffuse contribution throughout the Brillouin zone due to the increasing disorder in the magnitude of the displacements (see Fig. 5); (iii) at the transition it is likewise clear from Figs. 4 and 5 that the loss of long-range order and consequent rapid decrease in half-order intensity coincides with a rapid decrease in $\langle u^2 \rangle$ and concomitant gain in integer intensity; but (iv) the character of the simulated HT phase in the vicinity of the transition is clearly disordered, in that $\langle u^2 \rangle$ remains significantly larger than $\langle \Delta u^2 \rangle$; while (v) as the temperature increases above the transition, the integer beams begin to decrease in intensity again due now to the thermally driven increase of $\langle u^2 \rangle$ and $\langle \Delta u^2 \rangle$ that now resume.

This is essentially the character of the transition envisioned in an earlier approximate study of this short-range model,[17] with the refinement that we now have a detailed calculation of the variation of $\langle u^2 \rangle$ and the resultant effects on the integer beam intensities.

B. Role of wells at finite displacement in local potential

All of the features discussed in Sec. IV A are nonuniversal and thus dependent on the parameters in the model. (The one exception is the order-disorder character of the high-temperature phase in the immediate vicinity of the transition,[24] if it is second-order.) Thus it is interesting to consider the same features in model II, which has the same low-temperature distortion magnitude, but lacks minima at finite displacement in the local potential. In this case, the interactions not only determine the character of the ordered phase, but also drive the displacements. Figures 6 and 7 show plots for model II analogous to those of Figs. 4 and 5. Since T_c for model II is about $\frac{1}{2}$ that of model I the temperature scale has been expanded.

Although there are no obvious differences in the behavior of the order parameter between models I and II, it is clear that there is a quantitative difference at least in the behavior of the integer beams, due ultimately to the disparate behaviors of $\langle u^2 \rangle$ as seen in Figs. 5 and 7. In the latter case, the decrease of $\langle u^2 \rangle$ is nearly twice as large as the former between $T = 0$ and $T = T_c$, although even for model II the average displacement slightly above T_c is still about $0.56 u_0$, significantly larger than estimated normal thermal disorder.[20] A second difference can be seen by considering the ratio $\langle \Delta u^2 \rangle / \langle u^2 \rangle$. This quantity is small but increasing for both models below T_c. Well above T_c it is about 0.6 for model I and 0.8 for model II. These values both indicate a very disordered HT phase. To explicate its character a bit more clearly we have also used our simulation runs to obtain the distribution of values of $|u_x|$ and $|u_y|$ that occur at various temperatures in the two models. The results are shown in Figs. 8(a) and 8(b). We note that in both cases this distribution peaks at nonzero values at all temperatures shown, and as expected from Figs. 5 and 7, this peak value shifts in the direction of decreasing magnitude with increasing temperature. The shift is much more rapid in the case of model II and above T_c the relative weight of the small $|u_x|$ part of the distribution is much larger in model II than in model I. One should also note by examining the trend in Fig. 8(b) from T_c to $1.1 T_c$ to $1.3 T_c$ that the distribution function changes most rapidly in the range $(T_c, 1.1 T_c)$ and varies rather slowly above $1.1 T_c$.

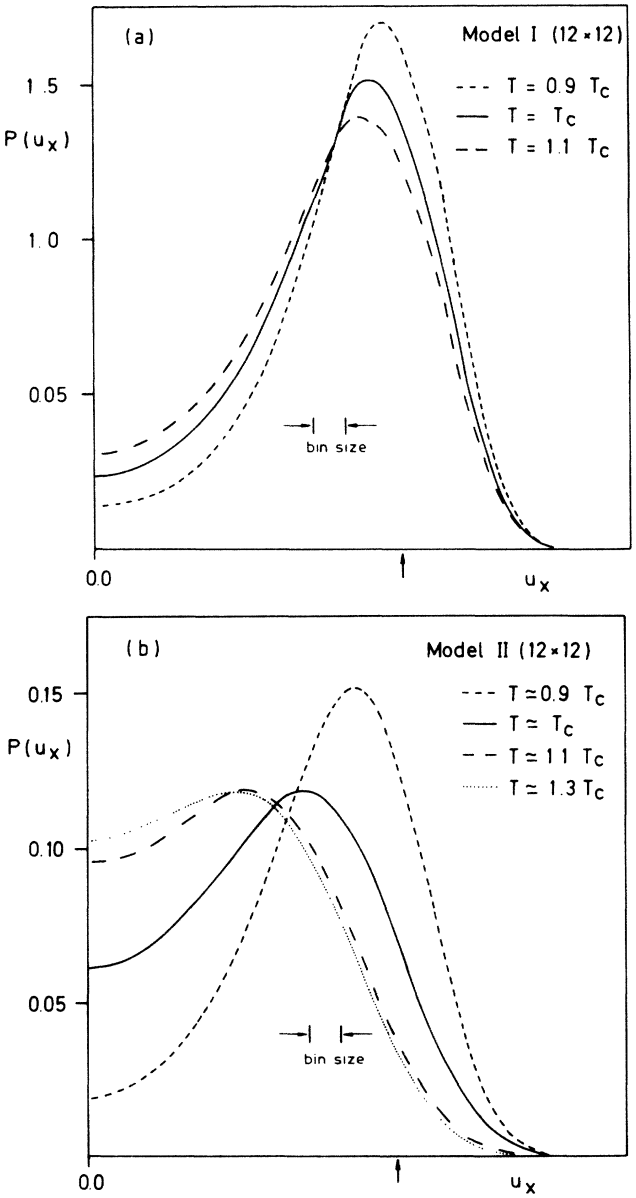

FIG. 8. Distribution of u_x values occurring in simulation of (a) model I, and (b) model II for various temperatures near T_c. The bin size of the histogram through which the smooth curves were drawn is indicated. The arrow denotes u_{0x}, the zero-temperature equilibrium value of u_x.

C. Character of the transition

A much more difficult question than the nature of the high-temperature phase of our model is the nature of the transition itself. Standard Landau classification[43] places both our model transition[3] and that of the actual system[44] in the universality class of the x-y model with cubic or four-fold anisotropy.[45] This, however, only tells us something if the transition turns out to be continuous. It is always possible that a transition classified as belonging to a universality class which displays continuous transitions, as does the x-y model, may still be superceded by a first-order transition. Although the experimental situation is not definite (see the discussion in the next section), the transitions appear to be second-order on the best surfaces[14] and the effect of steps on the transition[11-14] also suggests a transition in which the correlation length becomes very long (see next paper).

The main purpose of our work is not to elucidate the details of the critical behavior of this model, however interesting they are likely to be,[46] but instead to calculate nonuniversal properties amendable to experimental comparison and to determine the qualitative effect of various perturbations on the basic Hamiltonian. Nevertheless, at least the question of the order of the transition is of considerable importance, since exponents have been measured for the clean surface transition[14] and since the displacive view of this transition has been discussed[2,16] in terms of coexisting phases (nucleated by defects[1]) characteristic of a first-order transition.

We have accordingly examined the transition also on larger lattices, 24×24 and 48×48. The results for the order parameter for the three sizes are shown in Fig. 9. One sees the characteristic sharpening of the transition with increasing N. The ordering susceptibilities, i.e., the fluctuations in the half-order LEED intensity, plotted in Fig. 10, provide further indication. In a first-order transition one expects these susceptibilities to scale with system size,[47] i.e.,

$$\chi_{\max}(N) \propto N^{x} , \tag{4.1}$$

with $x=1$ in the large-N limit.

As one can see from Fig. 10, the behavior of the susceptibilities is consistent with $x<1$ implying a continuous transition. Some caution is in order, however. The 12×12 and 24×24 results are well converged with error bars about the size of the plotting symbols. The 48×48 results are less well converged, although it seems unlikely that the maximum in $\Delta I_{1/2,1/2}$ could in this case reach a maximum 16 times that of the 12×12 run (well off scale in Fig. 10). The error bar at $T=2.2$ is based on six sequential 20000 MC-step runs. In addition, the difficulty of finding the maximum of a sharply peaked function using noisy data at discrete intervals should not be minimized. Nonetheless, our conclusion is that the transition of model I appears to be continuous.

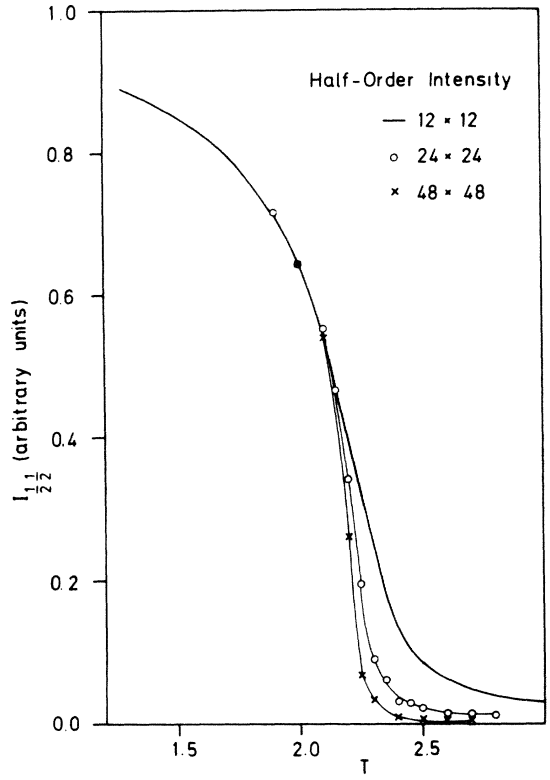

FIG. 9. Plots for model I showing the simulated, normalized (to 1.0 at $T=0$), kinematic half-order LEED intensity versus temperature for different lattice sizes. For clarity individual points from the (12×12) study are not included (see Fig. 4). The lines are drawn to guide the eye and have no further significance.

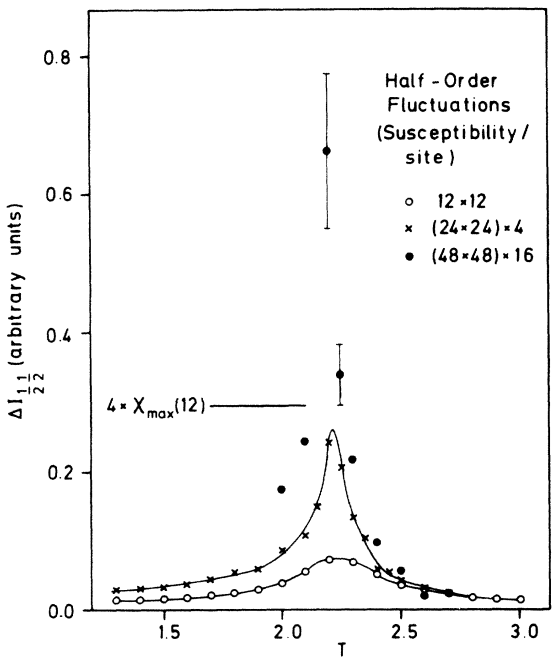

FIG. 10. Lattice size variation of the magnitude of the fluctuations in the kinematic half-order intensity per lattice site. The mark at 4 times the peak value of the 12×12 value represents the magnitude one would expect the 24×24 curve to obtain if the transition were first order.

V. DISCUSSION AND COMMENT ON EXPERIMENT

In this section we discuss the results presented in the last section more fully, particularly in the context of experimental results which are presented in this section and the limited experimental results which have been published previously. Implications for further study are also discussed.

A. Integer beams

The behavior of the integer beam going through the transition is important because, as emphasized by Debe and King,[16] this indicates whether a transition has order-disorder or displacive character (although we show this relationship to be less obvious than previously thought in light of the short-range interaction model). In the latter case, one expects in the kinematic approximation that the intensity which disappears from the half-order beam will reappear in the integer beams as the displacement magnitudes go to zero.[48] In the extreme order-disorder limit, in which the atomic displacements disorder but do not diminish in magnitude, one expects this intensity to be spread throughout the surface Brillouin zone. We begin by reviewing the available experimental information. Debe and King published the first study of the integer beams[16] in which the temperature dependences of the (00) beam at three different energies and that of the $(0\bar{1})$ beam at one energy were obtained. These data were invoked there and elsewhere[1,2,49] in support of the displacive picture of the transition. Strictly speaking, however, this interpretation has two difficulties. First, the variation of all four intensities shows a change in slope near the transition rather than an actual increase. Thus it might be more accurate to say (as pointed out in Ref. 22) that the Debye-Waller factor seems to vary in the vicinity of the transition, rather than that these data are direct evidence for a transition of displacive character. Heilmann, Heinz, and Müller[33] in fact determined a change in the surface Debye temperature (from 400 ± 100 K in the LT phase to 210 ± 40 K in the HT phase) of W(001) by studying the temperature and energy dependence of the (10) beam. Secondly, the (00) beam has momentum transfer totally in the z direction, i.e., perpendicular to the surface, and so is insensitive to variations in the x and y components of the surface atom displacements. One would thus expect for the specular beam *irrespective of the character of the transition,* to see exactly what is seen, i.e., at most a variation of the Debye-Waller factor.

In a recent study by Wendelken and Wang,[14] a more dramatic behavior of the integer-beam intensities was mentioned in connection with a study of the phase transition on a W(001) surface of exceptional quality. The integer-beam data mentioned in that study was not published there but is shown in Fig. 11 along with additional data. We attribute the differences in this data from that previously published primarily to the exceptionally large terrace widths which were determined to be greater than 400 Å (hence we refer to this surface as "flat"). In this recent study[14] it was shown that steps on the surface with an average terrace width of 30 Å could strongly influence the phase transition through finite-size effects.

Plotted in Fig. 11(a) is intensity versus temperature data for the $(\frac{1}{2},\frac{1}{2})$, (11), and (10) beams at an energy of 42 eV for the "flat" W(001) surface. The $(\frac{1}{2},\frac{1}{2})$ beam exhibits a local intensity maximum at this energy. An intensity gain in each of the integer beams is clearly observed to be correlated with the loss of intensity in the $(\frac{1}{2},\frac{1}{2})$ beam as the temperature is increased. The data were obtained by heating the sample to above 1000 K and then measuring

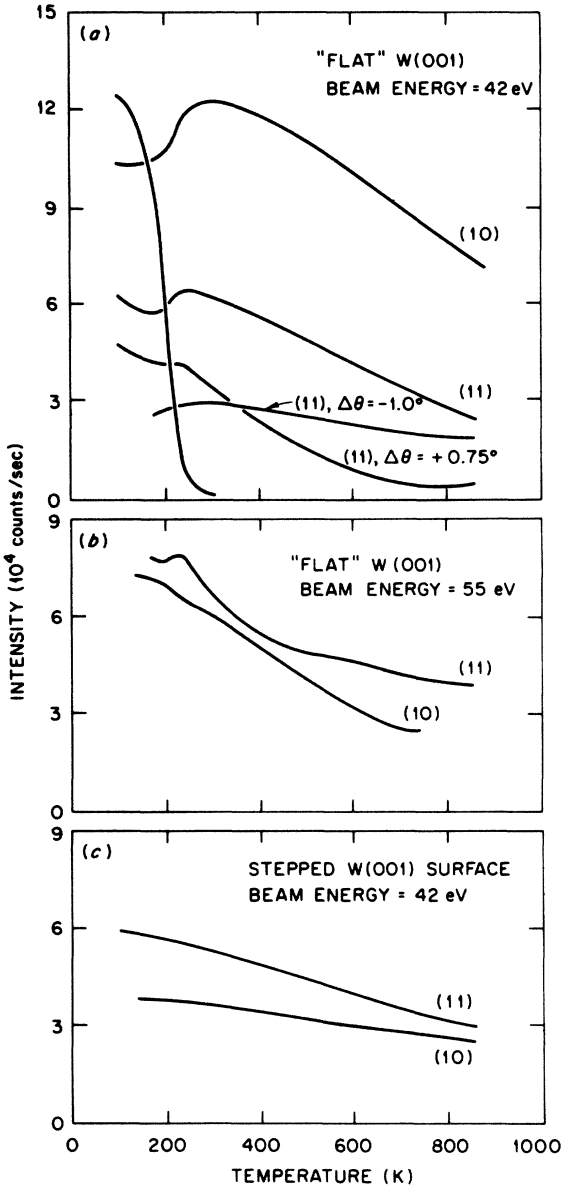

FIG. 11. Experimental measurements of electron diffraction intensities versus temperature for W(001). (a) A comparison of the (1/2,1/2), (11) and (10) beams at 42 eV for a "flat" surface (see text) which show clearly the intensity shift between the fractional order and integral order beams associated with the phase transition. In addition, measurements obtained at fixed angles of $-1.0°$ and $+0.75°$ relative to the beam angle at 100 K are shown for the (11) beam. (b) Measurements made of the (10) and (11) beams at an energy of 55 eV. (c) Measurements made of the (10) and (11) beams at an energy of 42 eV, but with a stepped surface with a 30 Å average terrace width.

the transient intensities as the sample cooled. Owing to the good angular resolution of the electron spectrometer used for these measurements ($<1.0°$ full width at half maximum), it was necessary to oscillate the detector in angle during the cooling cycle in order to track the beams which moved due to the thermal contraction of the cooling crystal and the small thermally induced distortions in the crystal mounting. The importance of this is indicated clearly in the lower two curves of Fig. 11(a), which were obtained for the (11) beam at fixed detector angles displaced $+0.75°$ and $-1.00°$ from the position in which the maximum intensity is obtained at 100 K.

In Fig. 11(b) additional data is shown for the (11) and (10) beams at an energy of 55 eV which corresponds to a minimum in the $(\frac{1}{2},\frac{1}{2})$ beam intensity. Note that in this case, the (10) beam is very insensitive to the phase transition with only a small change in the slope or Debye-Waller factor displayed. In fact, it is a general impression based on observations at other energies with this crystal as well as a second flat crystal which was prepared to similar standards, that the (10) beam is generally less sensitive than the (11) beam, but that the exact behavior is complex, probably due to multiple-scattering effects. The change in slope seen in Refs. 16 and 33 is present and qualitatively similar in our data as well, although it is difficult to make quantitative comparisons due to the variety of energies, beams, and temperature ranges employed for the different studies.

Measurements made with the 30-Å terrace-width crystal (referred to above[14]) of the (10) and (11) beams are shown in Fig. 11(c). In this case we see virtually no effect of the phase transition in the integer beams other than a very slight increase in intensity of the (11) beam at the phase transition and a very small change in the slope of the curves. We speculate that the small but genuine increase of intensity in the integer beams was smeared out in Debe and King's (01) beam data as a consequence of the 85-Å average-step separation of the crystal used in those measurements. (See the next paper for a discussion of the consequences of steps in our model.)

A glance back at Figs. 4 and 6 provides an explanation for some of the key experimental features. The increase in intensity in the vicinity of T_c is manifest in the simulations as a decrease in the magnitude of the integer-beam intensity loss, which occurs as a result of the decrease in $\langle u^2\rangle$ [see Figs. 5 and 7 and Eqs. (3.8)]. Note that Barker and Estrup[22] envisioned just such a decrease in $\langle u^2\rangle$ in their characterization of a disordered HT phase.

The decrease in $\langle u^2\rangle$ must be understood on the basis of the energetics specified by Eq. (2.7). It occurs because as order is lost the atom displacements partially lose the effect of the J_1 coupling [see Eq. (2.3a)] which tends to increase the magnitudes of the displacements when NN displacements are oppositely directed. This same mechanism should operate in the real surface as well.

The change in the *apparent* (see Sec. V B) Debye-Waller factor can also be readily understood at least for the nonspecular beams. Below T_c our simulation indicated that the integer beams actually increase in intensity as the temperature rises, gaining some, but not all, of the intensity lost by the half-order beams. This is due again mostly to the decrease in effectiveness of the *interaction term* as thermally induced disorder develops. In fact, the experimental (10) beam data shown in Fig. 11(a) appears to show this as a dominant effect, but the other beams observed only show a less negative slope below T_c. Well below T_c this disorder is primarily in the form of variations in displacement magnitude. (Note that if one displacement increases in magnitude to $u_0+\Delta$ and a neighbor decreased in magnitude to $u_0-\Delta$, their dot product *decreases* in magnitude, $u_0^2-\Delta^2$. Small variations in angle similarly decrease $|J_1 u_i\cdot u_j|$.) As the bond energy decreases in magnitude, $\langle u^2\rangle$ decreases and hence the integer intensity increases. Some of the loss of half-order intensity, however, is spread throughout the Brillouin zone because of the disorder in the surface layer. Near T_c this simple picture breaks down as the disorder becomes more varied and more extended in range. Above T_c, $\langle u^2\rangle$ begins to increase again due simply to thermal disorder. The result upon comparing the situation below and above T_c is a significant change in slope, besides the intensity increase at the transition. It is important to note that *in neither regime is this behavior the same as the classical Debye-Waller effect.* We return to this point in Sec. V B.

To understand why the slope of the specular beam also changes, we need to go beyond the physics included in our model, which allows only displacements in the surface plane. Allowing the displacements to have a z component as well would have two effects. First, there would be an additional Debye-Waller contribution affecting the intensity of each beam of the form

$$D_z(\Delta\mathbf{k})=\exp(-\Delta k_z^2\langle u_z^2\rangle)\,, \tag{5.1}$$

where $\Delta\mathbf{k}$ is the momentum transfer for the beam in question and Δk_z is its component normal to the surface. The specular and low-order integer beams have a relatively large Δk_z^2, so this factor would steepen the descent of all beams significantly and would also convert the increase seen in the integer beams in the simulation below T_c to a decrease. Secondly, Eq. (5.1) also allows an understanding of the experimentally observed change in slope for the specular beam. If motion in the z direction is completely uncoupled from motion in the surface plane, we would expect $\langle u_z^2\rangle$ to be simply proportional to temperature in line with equipartition of energy. However, it is entirely reasonable to suppose that the atoms move in a three-dimensional potential in which there is very strong coupling between u_z and (u_x,u_y). One can see this coupling directly in the slab electronic structure calculations of Fu *et al.*[6] (see especially their Fig. 3). Given this hypothesis, changes in $\langle u^2\rangle$ would drive similar rapid changes in $\langle u_z^2\rangle$, thus providing an explanation even for the change in slope of the specular beam. [In the kinematic approximation one could not, however, account for any increase in specular intensity like that which occurs for the (11) and (10) beams in Fig. 11(a) using this hypothesis.] Having accounted for the data we return to the issue of the character of the transition.

The terms "displacive" and "disordered" represent limiting cases of a rich spectrum of behavior. Neither case

can be perfectly realized in a model with short-range interactions. Perfect order-disorder behavior in which the displacement magnitudes remain constant cannot occur because disorder inherently decreases $\langle u^2 \rangle$. Perfect displacive behavior is also impossible because of the persistence of short-range order well above T_c,[14] again because of the interactions. (The temperature is high enough for long-range order to have been disrupted, but not so high as to make the Boltzmann factor for a NN bond negligible.) The factor which in large degree determines where in this spectrum a given model on the real system falls is the relative importance of the interactions [Eqs. (2.1) and (2.4)] *vis a vis* the local potential [Eq. (2.6)] in forming the reconstructed state. Our choices of models I and II are meant to roughly represent reasonable limits of this variation.

One might then be tempted to investigate the physics of the driving force by experimentally determining where on this spectrum the clean W(001) reconstruction transition falls. Model II would be consistent with a mechanism concentrated very much in the first layer. Model I would require some involvement in the driving force of the bulk, i.e., at least the second layer. Since slab-based electronic structure calculations are gaining in sophistication to the extent that total energies of various fully ordered phases can now be reliably calculated,[6] the time would seem to be propitious for such an undertaking. We caution, however, that to obtain information on this point from diffraction data like that of Fig. 11 will require very careful study of the effects of multiple scattering.

In the absence of such a careful study, there are indications that favor the model I end of the spectrum that should be mentioned. First, the IV profiles of the integer beams are remarkably similar (see Figs. 5 and 6 of Ref. 16) in the LT and HT phases. Although kinematically the magnitude of $\langle u^2 \rangle$ contributes only an overall normalization of the integer beam, certainly the multiple scattering will be influenced by the average magnitude of the displacements. Model II has $\langle u^2 \rangle$ decreasing by about $\frac{2}{3}$ between $T=0$ and $T \gtrsim T_c$ and by about $\frac{1}{2}$ between 10% below T_c and 10% above T_c. It is difficult to imagine such a large change not leading to some more significant changes in the IV profiles. The change in $\langle u^2 \rangle$, particularly in the transition region, is much more moderate for model I. A second indication is that the increase in integer-beam intensity associated with the transition is, in general, not dramatic, even though selected beams at appropriate energies show striking effects. Systematic measurements have not been carried out, but the impression remains that on average only a fraction of the half-order intensity is reappearing in the integer beams. The remaining intensity is presumed to go into momentum space as diffuse intensity. Preliminary measurements of the diffuse background have been obtained with the second flat W(001) crystal, and an example is shown in Fig. 12. These data, at 42 eV and with the same small solid angle as used for the beam studies, fail to show any sudden increase in diffuse intensity, but this is perhaps not surprising in light of the large solid angle involved and the relative magnitudes of the total diffuse intensity and the intensity lost from the half-order beams.

B. Implications of the variation of $\langle u^2 \rangle$ for measurement of critical phenomena and Debye-Waller effects

Interest in the experimental determination of critical exponents in a *bonafide* two-dimensional x-y model, of which the W(001) reconstruction is an example,[3,44] is great, since the model displays varying critical exponents[45] and a Kosterlitz-Thouless transition.[50] (Hydrogen absorption sweeps the anisotropy through zero,[3,9] thus rendering the K-T transition accessible.) Wendelken and Wang[14] have already reported a measurement of the order-parameter exponent β (result: $\beta=0.144\pm0.04$) for the clean surface reconstruction.

Technically, the pure x-y model with cubic anisotropy would correspond to displacements of fixed magnitude, and allowing them to fluctuate ("amplitude" fluctuations) is hoped to be irrelevant. Our study indicates that $\langle u^2 \rangle$ actually displays our energylike singularity and therefore should vary like

$$\langle u^2 \rangle \propto a + bt + c^{\pm} |t|^{1-\alpha} , \tag{5.2}$$

as do all short-range properties of a critical system[42,51] coupled to the energy. In Eq. (5.2),

$$t=(T-T_c)/T_c , \tag{5.3}$$

and a, b, and $c^{\pm}$ are constants, the latter having possibly different values above and below T_c. In the case of an Ising transition (which occurs for large anisotropy in the x-y model[3,45]) the $|t|^{1-\alpha}$ term is replaced by $|t| \ln |t|$.

The average displacement magnitude, determined from $\langle u^2 \rangle$, factors into the half-order beam intensity, as a normalization constant. This means that in contrast to the situation in a lattice gas,[52] the half-order kinematic intensity is no longer proportional to the squared order parameter. Instead, even if amplitude fluctuations are ir-

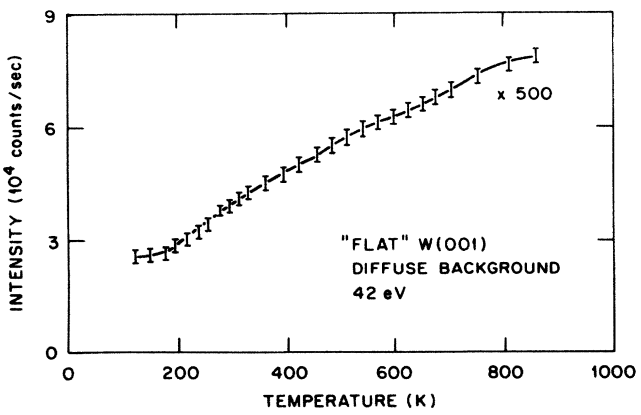

FIG. 12. Background diffuse scattering intensity measurement at 42 eV in a random direction with a second "flat" W(001) crystal.

relevant, there will be a singular correction near T_c:

$$I_{1/2,1/2} \propto \langle u^2 \rangle M^2 , \tag{5.4}$$

of an x-y model without amplitude fluctuations, where M is the order parameter. In general, M should vary like

$$M \propto |t|^{\beta} \tag{5.5}$$

below T_c. Combining Eqs. (5.2), (5.4), and (5.5) indicates that there will be new corrections to scaling that below T_c will have the form

$$I_{1/2,1/2} = \tilde{a} |t|^{2\beta} + \tilde{c}^{-} |t|^{2\beta+1-\alpha} \tag{5.6}$$

in a very large system so that critical scattering contributes negligibly. $\tilde{a}$ and $\tilde{c}^{-}$ are constants. The correction obviously becomes relatively more important as one moves away from T_c, limiting the range over which one can expect simple power-law behavior.[53]

Finally we raise the issue of the nature of Debye-Waller effects in this system. The classical Debye-Waller effect[27] refers to loss of coherent diffracted intensity due to increasing thermal disorder which takes the form

$$\langle u^2 \rangle \propto T \tag{5.7}$$

in a simple harmonic crystal. We have demonstrated that at least for $\langle u_x^2 + u_y^2 \rangle$ one has for the W(001) surface a temperature dependence drastically different from Eq. (5.7). [Equation (5.2) is a better description throughout the entire temperature range we studied.] Besides the significance for the analysis of critical exponent data there are also obvious implications for the analysis of ion-scattering data[34] (where a key role in the analysis is played by Debye-Waller effects[35]), and dynamical LEED analysis of the HT phase (see Sec. I B). If our model of the surface atom behavior is realistic, the treatment of the Debye-Waller effects in Ref. 49, being based on a simple independent oscillator approach, is entirely misleading.[54]

VI. SUMMARY

In this paper we have extended an earlier study of short-range interaction models for surface reconstructions[7] to now include two-dimensional displacements and four-fold symmetry appropriate for discussing the clean W(001) transition. We have also presented important new data for the behavior of the integer diffraction beams near the transition. In reconciling these experimental results with our simulations of the short-range models we have achieved an important new understanding of the nature of the W(001) reconstruction transition and its high-temperature phase. The key points include (i) a model with short-range interactions always displays a disordered phase near and somewhat above the transition; (ii) parameter choices that encompass the conceivable variations in the physics of the driving force lead to high-temperature phases with a high degree of disorder, although the average magnitude of displacement does vary significantly between these limits; (iii) current experimental indications seem more consistent with the model displacing larger displacements in the high-temperature phase, implying that interactions with second-layer W atoms are significant in the driving force; (iv) variations of the average displacement magnitude also contribute corrections to scaling in LEED-derived measurements of the phase transition order parameter; and (v) the W(001) surface displays anomalous Debye-Waller behavior.

We should also point out the limitations of this study. The range of interaction on this surface has not been adequately established. Inglesfield[1] has, for example, estimated a range of 10 Å, though presumably due to the almost chemical nature of the driving force, the dominant part of the effect occurs at shorter range. A second issue is that the validity of the small displacement approximation which allows one to write the interaction as quadratic forms in the displacements [Eqs. (2.1) and (2.6)] has not been established. In this context we mention that the dependence of the total energy on displacement magnitude as calculated by Fu *et al.*[6] displays an initial small increase before a decrease of about 0.01 eV to a minimum at $u_0 = 0.18$ Å.[55] If the initial small increase in energy is real, then fourth-order terms in the interactions may be significant and sixth-order terms would be needed in the local potential to bound the displacements. Inclusion of such terms in the simulation would be straightforward and we would not expect our conclusions to be altered. However, the increase in the number of parameters needed to fully characterize the driving force would be quite unpleasant. We should also mention that the decrease of the correlation length in the real system—as seen in the beam width plot of Ref. 14—is more rapid than for model I above the transition. Ying[25] has noted that the correlations become more persistent as the magnitude of the anisotropy, V_4, decreases. This seems to us a promising approach for estimating the strength of the anisotropy in the real system.

Finally, it must be acknowledged that multiple-scattering complications have not been dealt with in our study. One could imagine that the experimental increase of integer intensity is a multiple-scattering effect due to say a variation in the last layer spacing concurrent with the transition. This seems quite unlikely to us, for the following reason. If this were a multiple-scattering effect one would expect that at some energies an intensity *decrease* would occur coincidentally with the transition, as the effect would be as likely to result in destructive changes as it would in constructive changes in interference. We have, however, never seen a decrease, despite having measured the temperature dependence at a moderate number of energies.

In the following paper we take up two other important questions that bear on the consistency between our short-range interaction model and experiment, the effect of steps on the transition and the effect of "perturbation terms" not included in the simulations presented here but allowed by symmetry. This latter topic is also important in the context of the effect of adsorption on the reconstruction.

ACKNOWLEDGMENTS

We acknowledge very helpful discussions with P. J. Estrup, J. E. Inglesfield, D. A. King, G.-C. Wang, R. Willis, and S.-C. Ying. We are also grateful to N. V. Richardson (Ref. 38) and J. E. Inglesfield (Ref. 1) for providing copies of their work prior to publication. S.-C. Ying provided a very useful critique of an early version of this paper. A. Preusser was of great assistance in managing the extensive computing entailed by this project.

---

*Permanent address: Department of Physics, Haverford College, Haverford, PA 19041.

[1]J. E. Inglesfield, Progr. Surf. Sci. **20**, 105 (1985).

[2]D. A. King, Phys. Scr. **T4**, 34 (1983).

[3]S. C. Ying and L. D. Roelofs, Surf. Sci. **125**, 218 (1983).

[4]K. Terakura, I. Terakura, and Y. Teraoka, Surf. Sci. **86**, 535 (1979); K. Terakura, I. Terakura, and N. Hamada, *ibid.* **103**, 103 (1981); I. Terakura, K. Terakura, and N. Hamada, *ibid.* **111**, 479 (1981).

[5]L. F. Mattheiss and D. R. Hamann, Phys. Rev. B **29**, 5372 (1984).

[6]C. L. Fu, A. J. Freeman, E. Wimmer, and M. Weinert, Phys. Rev. Lett. **54**, 2261 (1985).

[7]L. D. Roelofs, G. Y. Hu, and S. C. Ying, Phys. Rev. B **28**, 6369 (1983).

[8]K. H. Lau and S. C. Ying, Phys. Rev. Lett. **44**, 1222 (1980).

[9]L. D. Roelofs and S. C. Ying, Surf. Sci. **147**, 203 (1984).

[10]L. D. Roelofs, J. W. Chung, S. C. Ying, and P. J. Estrup, Phys. Rev. B **33**, 6537 (1986).

[11]J. F. Wendelken and G.-C. Wang, J. Vac. Sci. Technol. A **2**, 888 (1984).

[12]J. F. Wendelken and G.-C. Wang, Surf. Sci. **140**, 425 (1984).

[13]G.-C. Wang and T.-M. Lu, Surf. Sci. **122**, L635 (1982).

[14]J. F. Wendelken and G.-C. Wang, Phys. Rev. B **32**, 7542 (1985).

[15]M. K. Debe and D. A. King, Phys. Rev. Lett. **39**, 708 (1977).

[16]M. K. Debe and D. A. King, Surf. Sci. **81**, 193 (1979).

[17]R. A. Barker, P. J. Estrup, F. Jona, and P. M. Marcus, Solid State Commun. **25**, 375 (1978).

[18]J. A. Walker, M. K. Debe, and D. A. King, Surf. Sci. **104**, 405 (1981).

[19]It should be noted, however, that a significant discrepancy remains in the last layer spacing. The total-energy calculation suggests little change from the bulk value while experiment (Ref. 18) indicates a 6% contraction.

[20]It is not simple to arrive at an estimate of the thermal vibration amplitude of the surface atoms. Simple harmonic theory—A. A. Maradudin, E. W. Montroll, G. H. Weiss, and I. P. Ipatova, *Theory of Lattice Dynamics in the Harmonic Approximation* (Academic, New York, 1971), Suppl. 3—suggests that surface amplitudes will be greater than bulk amplitudes by a factor of $\sqrt{2}$. I. Stensgaard, L. C. Feldman, and P. J. Silverman, Surf. Sci. **77**, 513 (1978), quote a value of $\rho=0.063$ Å for the two-dimensional bulk root-mean-square displacement of W. A simple Debye theory calculation based on the tabulated [G. T. Furukawa and T. B. Douglas, in *American Institute of Physics Handbook*, 3rd ed., edited by D. E. Gray (McGraw-Hill, New York, 1972)] value of $\Theta_{\text{Debye}}=400$ K gives a result of $\rho=0.04$ Å. Thus $\rho_{\text{surf}}=0.07\pm0.02$ Å might be a reasonable compromise estimate.

[21]M. K. Debe and D. A. King, J. Phys. C **15**, 2257 (1982).

[22]R. A. Barker and P. J. Estrup, J. Chem. Phys. **74**, 1442 (1981).

[23]E. Stoll and T. Schneider, in *Solitons and Condensed Matter Physics*, edited by A. R. Bishop and T. Schneider (Springer, New York, 1978).

[24]A. D. Bruce and R. A. Cowley, Adv. Phys. **29**, 219 (1980).

[25]S. C. Ying, in *Dynamical Phenomena at Surfaces, Interfaces and Superlattices*, edited by F. Nizzoli, K.-H. Rieder, and R. W. Willis (Springer, Berlin, 1985), p. 148.

[26]S. Ohnishi, A. J. Freeman, and E. Wimmer, Phys. Rev. B **29**, 5267 (1984).

[27]J. B. Pendry, *Low Energy Electron Diffraction* (Academic, London, 1974).

[28]C. Guillot, M. C. Desjonquères, D. Chaveau, G. Tréglia, J. Lecante, D. Spanjaard, and Tran Minh Duc, Solid State Commun. **50**, 393 (1984).

[29]C. Guillot, C. Thuault, Y. Jugnet, D. Chaveau, R. Hoogewijs, J. Lecante, Tran Minh Duc, G. Treglia, M. C. Desjonqueres, and D. Spanjaard, J. Phys. C **15**, 4023 (1982).

[30]In the $c(2\times2)$-H phase the surface atoms are displaced as in Fig. 1(e) with H atoms adsorbed onto the pinched bridge sites. See Ref. 22 and references therein.

[31]J. C. Campuzano, J. E. Inglesfield, D. A. King, and C. Somerton, J. Phys. C **14**, 3099 (1981).

[32]M. I. Holmes and T. Gustafsson, Phys. Rev. Lett. **47**, 443 (1981).

[33]P. Heilmann, K. Heinz, and K. Müller, Surf. Sci. **89**, 84 (1979).

[34]I. Stensgaard, L. C. Feldman, and P. J. Silverman, Phys. Rev. Lett. **42**, 247 (1979).

[35]J. F. Van der Veen, Surf. Sci. Rep. **5**, 199 (1985).

[36]L. D. Roelofs, Surf. Sci. (to be published).

[37]D. P. Woodruff, Surf. Sci. **122**, L635 (1983).

[38]S. M. Francis and N. V. Richardson, Phys. Rev. B **33**, 662 (1986); J. W. Chung, S.-C. Ying, and P. J. Estrup, Phys. Rev. Lett. **56**, 749 (1986).

[39]K. Binder, in *Monte Carlo Methods in Statistical Physics*, edited by K. Binder (Springer, Berlin, 1979), p. 1.

[40]L. D. Roelofs, in *Chemistry and Physics of Solid Surfaces, IV*, edited by R. Vanselow and R. Howe (Springer, Berlin, 1982), p. 219.

[41]J. M. Phillips, L. W. Bruch, and R. D. Murphy, J. Chem. Phys. **75**, 5097 (1982); Vacuum **34**, 579 (1984).

[42]N. C. Bartelt, T. L. Einstein, and L. D. Roelofs, Surf. Sci. **149**, L47 (1985); Phys. Rev. B **32**, 2993 (1985).

[43]M. Schick, Progr. Surf. Sci. **11**, 245 (1981).

[44]P. Bak, Solid State Commun. **32**, 581 (1979).

[45]J. V. Jose, L. P. Kadanoff, S. Kirkpatrick, and D. R. Nelson, Phys. Rev. B **16**, 1217 (1977).

[46]The x-y model with four-fold anisotropy displays "nonuniversal" critical exponents. See Ref. 45.

[47]P. Kleban and C. K. Hu (unpublished).

[48]The important quantity is not actually the displacement magnitudes, but instead, their degree of uniformity. Thus, ordered phases of any character, including those of Figs. 1(a) and 1(b) lead to no loss of integer-beam intensity, as can readily be seen using Eqs. (3.8a) and (3.8b).

[49]T. Matsubara, in *Dynamical Processes and Ordering on Solid Surfaces,* edited by Y. Yoshimori and M. Tsukada (Springer-Verlag, Berlin, 1985), p. 180.

[50]J. M. Kosterlitz and D. J. Thouless, J. Phys. C **6**, 1181 (1973); J. M. Kosterlitz, *ibid.* **7**, 1046 (1974).

[51]M. E. Fisher and J. S. Langer, Phys. Rev. Lett. **20**, 665 (1968).

[52]T. L. Einstein, in *Chemistry and Physics of Solid Surfaces VI,* edited by R. Vanselow and R. Howe (Springer, Berlin, 1982), p. 251.

[53]Even in lattice gas systems there are corrections to scaling intrinsic to the critical behavior below T_c which must be taken into account when analyzing LEED data. See N. C. Bartelt, T. L. Einstein, and L. D. Roelofs (unpublished).

[54]It is also worth noting that the identification of T_c with the temperature at which one finds some curvature in the plot of integer beams in Ref. 49 is totally incorrect as can readily be seen from an examination of Fig. 11.

[55]Interestingly, an earlier study—G. Treglia, M.-C. Desjonqueres, and D. Spanjaard, J. Phys. C **16**, 2407 (1983)—which concluded that the undistorted phase was lower in energy than the $c(2\times2)$ phase of Fig. 1(d), was based on a comparison of total energies at displacements of 0.0 and 0.08 Å. At 0.08 Å, Fu *et al.* (Ref. 6) also find that the $c(2\times2)$ phase is higher in energy, though by a smaller amount.

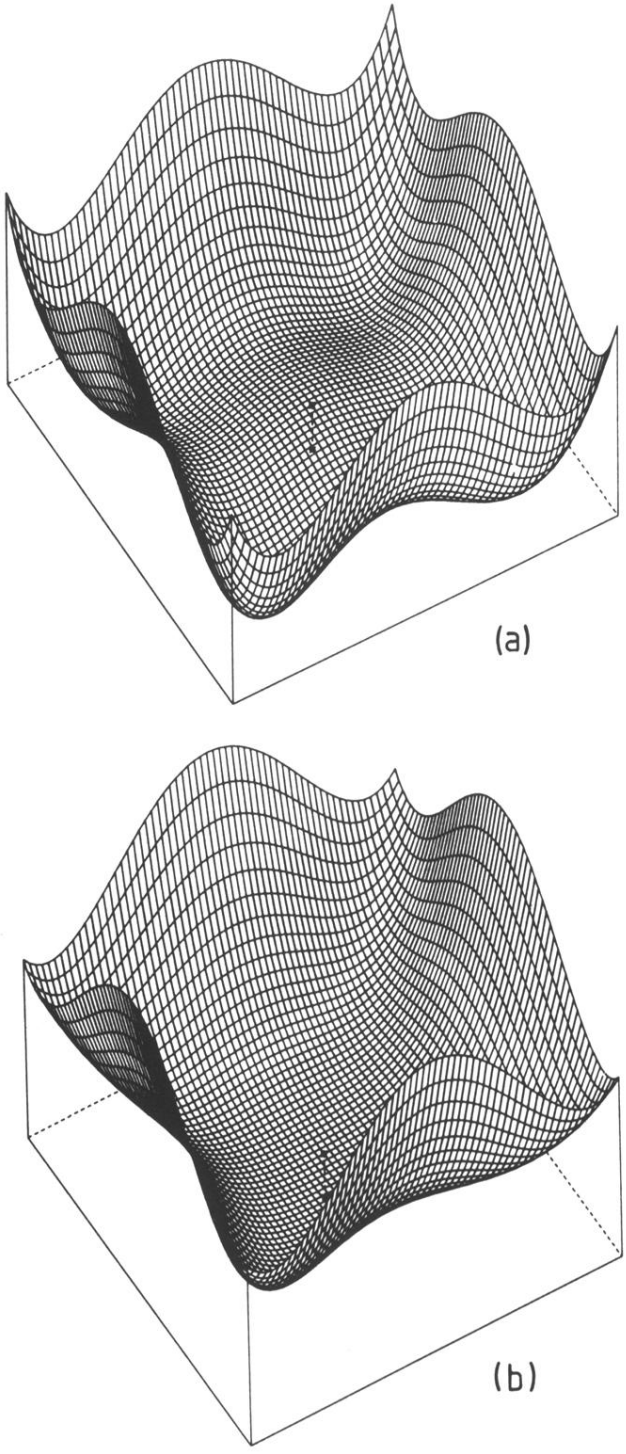

FIG. 3. Plot of assumed local potentials for (a) (top) model I and (b) (bottom) model II. $V(u_x,u_y)$ is represented by the vertical direction and the square beneath each plot is oriented with its edges along the $\langle 100 \rangle$ and $\langle 010 \rangle$ directions.